—Original Article—

Quantitative evaluation of cervical cord compression by computed tomographic myelography in Thoroughbred foals

Kazutaka YAMADA[1,4]*, Fumio SATO[2], Tetsuro HADA[2], Noriyuki HORIUCHI[1], Hiroki IKEDA[3], Kahori NISHIHARA[1], Naoki SASAKI[1], Yoshiyasu KOBAYASHI[1] and Yasuo NAMBO[1]

[1]Obihiro University of Agriculture and Veterinary Medicine, Hokkaido 080-8555, Japan
[2]Hidaka Training and Research Center, Japan Racing Association, Hokkaido 057-0171, Japan
[3]Hidaka Horse Breeders Association, Hokkaido 056-0002, Japan
[4]Present affiliation: Azabu University, Kanagawa 252-5201, Japan

Five Thoroughbred foals (age, 8–33 weeks; median age, 31 weeks; weight, 122–270 kg; median weight, 249 kg) exhibiting ataxia with suspected cervical myelopathy (n=4) and limb malformation (n=1) were subjected to computed tomographic (CT) myelography. The areas of the subarachnoid space and cervical cord were measured on transverse CT images. The area of the cervical cord was divided by the area of subarachnoid space, and stenosis ratios were quantitatively evaluated and compared on the basis of histopathological examination. The sites with a ratio above 52.8% could have been primary lesion sites in the histopathological examination, although one site with a ratio of 54.1% was not a primary lesion site. Therefore, in this study, a ratio between 52.8–54.1% was suggested to be borderline for physical compression that damages the cervical cord. All the cervical vertebrae could not be scanned in three of the five cases. Therefore, CT myelography is not a suitable method for locating the site of compression, but it should be used for quantitative evaluation of cervical stenosis diagnosed by conventional myelography. In conclusion, the stenosis ratios determined using CT myelography could be applicable for detecting primary lesion sites in the cervical cord.

Key words: *cervical vertebral compressive myelopathy, computed tomographic myelography, contrast agent, quantitative evaluation, Thoroughbred*

J. Equine Sci.
Vol. 27, No. 4
pp. 143–148, 2016

Cervical vertebral compressive myelopathy is a primary concern in ataxic horses and has a higher incidence in Thoroughbreds; it is typically seen in young, rapidly growing horses demonstrating evidence of developmental orthopedic disease. This condition is also commonly associated with a poor prognosis for racing and consequent economic loss [5]. It is more likely a multifactorial disease that involves influences, such as environmental, genetic, dietary, and traumatic events, with rapidly growing individuals being at a higher risk [13]. In humans, cervical myelopathy appears in adolescent athletes, and it is considered that excessive training, rather than muscle development, may predispose humans for this condition.

X-ray examination is the first diagnostic tool of choice for the diagnosis of orthopedic disorders. Radiographic findings, including subluxation, apparent extension of the vertebral arch, dorsal projection of the caudal epiphysis, and articular process osteophytes, can suggest a cervical abnormality [8, 13]. However, cord compression cannot be identified based on survey radiographs; therefore, myelography has long been recognized as the method used to determine if spinal cord compression is present [1, 10, 13]. A lateral cervical myelogram can reveal the site and degree of compression, but its interpretation is somewhat subjective. Equine computed tomography (CT) was first introduced in 1987 [3]. While CT requires general anesthesia, the cross-sectional images enable us to calculate the ratio of the areas of the subarachnoid space and cervical cord for a more accurate quantitative evaluation. Janes *et al*. reported quantitative evaluation by magnetic resonance imaging (MRI) [7] with

Received: February 1, 2016
Accepted: May 18, 2016
*Corresponding author. e-mail: kyamada@azabu-u.ac.jp

Table 1. Case descriptions for computed tomographic myelography

	Age (weeks)	Sex	Breed	Body weight (kg)	Symptom
Case 1	30	Female	Thoroughbred	209	Ataxia since 16 weeks of age
Case 2	31	Male	Thoroughbred	249	Ataxia since 16 weeks of age
Case 3	33	Female	Thoroughbred	262	Ataxia since 24 weeks of age
Case 4	32	Female	Thoroughbred	270	Ataxia since 24 weeks of age
Case 5	8	Male	Thoroughbred	122	Limb malformation

Fig. 1. Photograph of the computed tomography examination of a foal.

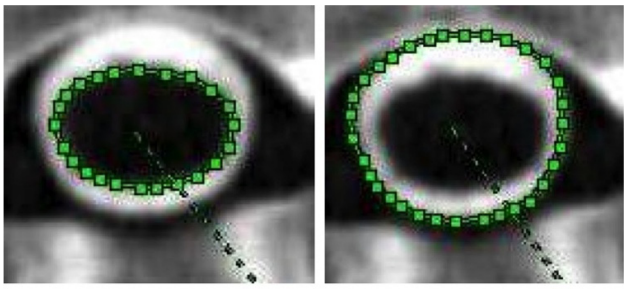

Fig. 2. Measurement area of the cervical cord and subarachnoid space on a transverse computed tomography myelogram.

a concept similar to the one presented here. We investigated an objective number of stenosis ratios and established a quantitative evaluation method using CT myelography.

Materials and Methods

Cases

Five Thoroughbred foals (age, 8–33 weeks; median age, 31 weeks; weight, 122–270 kg; median weight, 249 kg) exhibiting ataxia with suspected cervical myelopathy (n=4) and limb malformation (n=1) due to poor prognosis for athletic performance were used in this study. Case descriptions are listed in Table 1. The study protocol was approved by the Animal Experiment and Welfare Committee of Obihiro University of Agriculture and Veterinary Medicine.

CT myelography

Foals were premedicated with medetomidine (5 μg/kg, intravenous [i.v.]), and guaifenesin (25–50 mg/kg, i.v.) was rapidly infused until the horse became ataxic. Anesthesia was induced with thiamylal sodium (4 mg/kg, i.v.) and diazepam (30 μg/kg, i.v.) and was maintained with a triple drip containing guaifenesin at a rate of 200 mg/kg/hr. An 18 gauge spinal needle was placed into the subarachnoid space via the atlanto-occipital junction. Cerebrospinal fluid was withdrawn over 2 min, 100 m*l* of contrast agent (iohexol, 140 mgI/m*l*, Teva Pharmaceutical Industries, Tokyo, Japan) was injected into the subarachnoid space, and then the foals were set in the supine position on a large animal patient table (Fig. 1). CT myelograms were obtained with a tube voltage of 135 kV, tube current of 150 mA, slice thickness of 1.0 mm, and helical pitch of 5.0 using 4-row multidetector CT (Asteion Super4, Toshiba, Tokyo, Japan), and sagittal images were fixed using curved multi-planar reconstruction image-processing software (VirtualPlace, Aze, Tokyo, Japan). The areas of the subarachnoid space and cervical cord were measured in transverse images. The area of the cervical cord was divided by the area of the subarachnoid space, and the stenosis ratio was calculated (Fig. 2).

Pathological examination

The horses were euthanized, and they underwent a necropsy after a complete CT examination. The cervical cord was collected, fixed in 15% neutral buffered formalin, cut into transverse sections, embedded in paraffin, and cut into 5-μm-thick sections. The paraffin-embedded sections were stained with hematoxylin and eosin for histopathological analysis.

Results

Diagnostic CT myelograms from C1–7 were obtained in cases 1 and 5, but CT myelograms only up until C5 were obtained in cases 2, 3, and 4. This was due to a limitation in scanning all the cervical vertebrae using this CT unit.

Cases

Case 1: The cervical cord was compressed at the levels of C3–4 in the CT myelogram (Fig. 3). The ratio of cervical stenosis was 61.3% (Table 2).

Case 2: The cervical cord was compressed at the levels of C2–3, C3–4, and C4–5 in the CT myelogram (Fig. 4); the ratios of cervical stenosis were 47.2, 46.3, and 43.5%, respectively (Table 3).

Case 3: The cervical cord was compressed at the level of C3–4 in the CT myelogram. Prominent subdural leakage showing an undulating margin was observed from C1 to C4 in the CT myelogram (Fig. 5). The ratio of cervical stenosis was 52.8% at the level of C3–4. Moreover, the ratios of cervical stenosis at the levels of C2–3 and C4–5 at the subdural leakage sites were 60.7% and 63.0%, respectively (Table 4).

Case 4: The cervical cord was compressed at the level of C3–4 in the CT myelogram (Fig. 6). The ratio of cervical stenosis was 63.7% (Table 5).

Case 5: The cervical cord was compressed at the level of C2–3 and C3–4 in the CT myelogram (Fig. 7). The ratios of cervical stenosis were 52.2% and 48.7%, respectively (Table 6).

Pathological examination

Microscopically, cases 1, 3 and 4 exhibited axonal

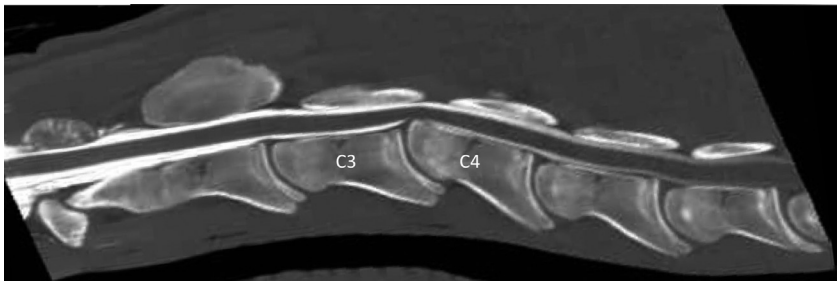

Fig. 3. Computed tomography myelogram of case 1. The cervical cord was compressed at the level of C3–4.

Table 2. Ratios of the areas of the subarachnoid space and cervical cord on transverse images in case 1

	C1–2	C2–3	C3–4	C4–5	C5–6	C6–7
Area of subarachnoid space (mm^2)	326	269	155	271	297	338
Area of cervical cord (mm^2)	116	120	95	122	129	156
Ratio (%)	35.6	44.6	61.3	45.0	43.4	46.2

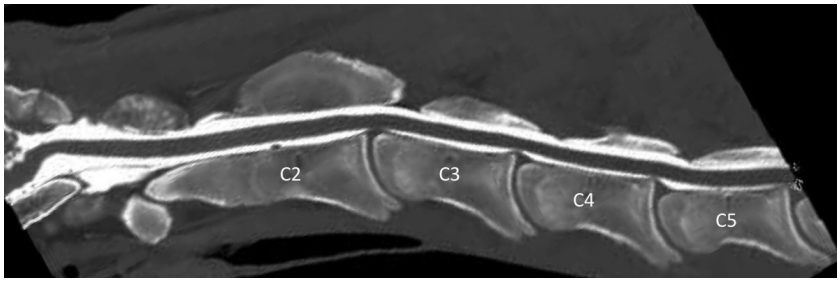

Fig. 4. Computed tomography myelogram of case 2. The cervical cord was compressed at the levels of C2–3, C3–4, and C4–5.

Table 3. Ratios of the areas of the subarachnoid space and cervical cord on transverse images in case 2

	C1–2	C2–3	C3–4	C4–5
Area of subarachnoid space (mm^2)	303	235	244	315
Area of cervical cord (mm^2)	123	111	113	137
Ratio (%)	40.6	47.2	46.3	43.5

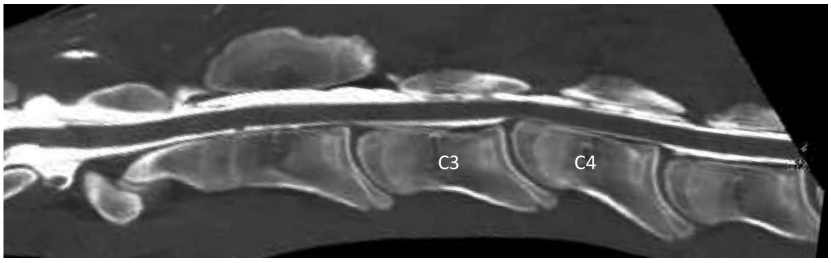

Fig. 5. Computed tomography myelogram of case 3. The cervical cord was compressed at the level of C3–4.

Table 4. Ratios of the areas of the subarachnoid space and cervical cord on transverse images in case 3

	C1−2	C2−3	C3−4	C4−5
Area of subarachnoid space (mm^2)	294	173	218	189
Area of cervical cord (mm^2)	136	105	115	119
Ratio (%)	46.3	60.7*	52.8	63.0*

*Severe subdural leakage.

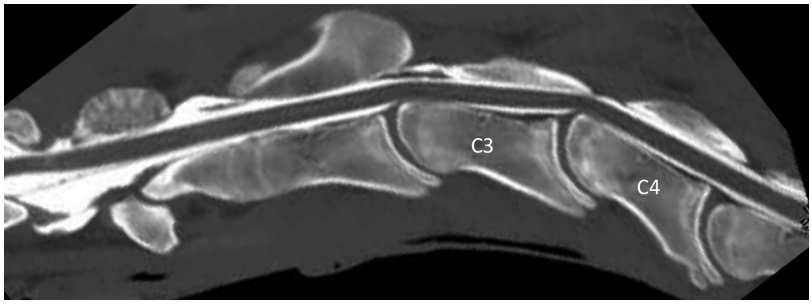

Fig. 6. Computed tomography myelogram of case 4. The cervical cord was compressed at the level of C3–4.

Table 5. Ratios of the areas of the subarachnoid space and cervical cord on transverse images in case 4

	C1−2	C2−3	C3−4	C4−5
Area of subarachnoid space (mm^2)	286	207	146	275
Area of cervical cord (mm^2)	115	112	93	123
Ratio (%)	40.2	54.1	63.7	44.7

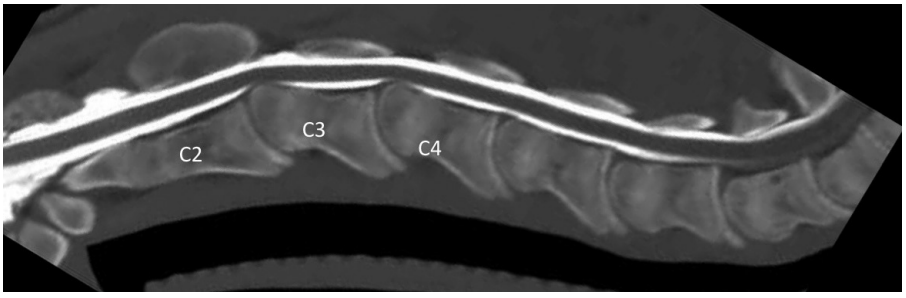

Fig. 7. Computed tomography myelogram of case 5. The cervical cord was compressed at the levels of C2–3 and C3–4.

Table 6. Ratios of the areas of the subarachnoid space and cervical cord on transverse images in case 5

	C1−2	C2−3	C3−4	C4−5	C5−6	C6−7
Area of subarachnoid space (mm^2)	309	201	236	265	283	331
Area of cervical cord (mm^2)	119	105	115	115	125	137
Ratio (%)	38.5	52.2	48.7	43.4	44.2	41.4

degeneration and secondary demyelination (Fig. 8), and the patterns of distribution of the axonal lesions matched the pattern of the neuropathologic lesions because of compressive myelopathy [4]. And the primary lesion site, at which the spinal cord was physically compressed, was estimated to be C3–4 in case 1, C3–4 in case 3, and C3–4 in case 4 because of the diffused axonal disruption at the site.

Discussion

Cervical myelopathy progresses often irreversibly, and therefore, it needs to be diagnosed in the early stages. To clarify the prognosis, several methods have been reported to achieve an objective evaluation. Scoring methods, such as use of the intervertebral sagittal ratio [6], have been reported that use radiographs to evaluate spinal canal stenosis but not spinal cord compression [8, 9, 13]. For more accuracy, myelography can show the reduction of the dual sac. From a technical viewpoint, the advantage, especially with the use of "standing" myelography, is that general anesthesia is not required [10], and ultrasound guidance minimizes accidental insertion of a needle into the spinal cord [2]. However, even in myelography, variability is present [5]. The CT myelogram is sensitive to lesions, but it can obtain only static images, whereas dynamic myelograms can obtain images in flexion and extension. In addition, even in a diagnostic CT myelogram, interpretation is somewhat subjective. Therefore, it is necessary to establish an objective quantitative evaluation method. Sites with a ratio above 52.8% could have been primary lesion sites in the histopathological examination, although one site with a ratio of 54.1% (case 4) was not a primary lesion site. Therefore, a ratio between 52.8–54.1% was suggested to be borderline for physical compression that damages the cervical cord in this study. In summary, quantitative evaluation of cervical stenosis was applicable for detecting primary lesion sites of the spinal cord.

In case 3, the stenosis ratios at C2–3 and C4–5 were 60.7% and 63.0%, respectively. This case presented prominent subdural contrast leakage and compressed subarachnoid space, making the areas of subarachnoid space relatively small. Therefore, the measured ratios were large and affected the subsequent quantitative evaluation. Occasionally, there was unintentional injection of the contrast agent into the outer subarachnoid space via subdural injection. Although we used an 18 gauge needle in this study, a smaller needle (e.g., a 20 gauge needle) may reduce the incidence of subdural injection [11].

In case 5, there was compression at the levels of C2–3 and C3–4, and the ratios were 52.2% and 48.7%, respectively. This case exhibited limb malformation, but neurological deficits suspected to be due to cervical myelopathy were not observed. Moreover, no significant lesions were detected even in the histopathological examination. Therefore, the compressions observed in the sagittal CT images and stenosis ratio of 52.2% were considered to be within the normal range.

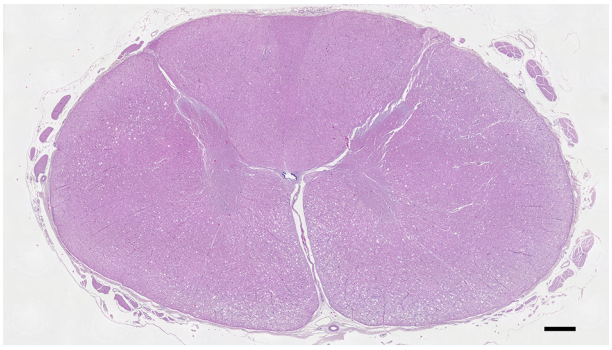

Fig. 8. Representative cross section of a spinal cord at C3–4 (case 1). Hematoxylin eosin stain. Bar, 1,000 μm.

It has been reported that the most common site of a cervical vertebral compressive lesion is the caudal vertebrae, including C5–6 and C6–7 [8]. In this study, the sites of compression and pathological changes were at the level of C3–4 in cases 1, 3, and 4. However, for cases 2, 3, and 4, all the cervical vertebrae could not be scanned. Therefore, the stenosis ratios at the levels of C5–6 and C6–7 remain unknown, and the predilection of the compression site warrants further investigation. The diameter of the CT gantry used in this study was 72 cm, which is the limit for scanning all the cervical vertebrae, even in foals. Thus, CT myelography is not suitable for locating the site of compression, and it should be used for quantitative evaluation of cervical stenosis diagnosed by conventional myelography. The development of a wide gantry CT capable of evaluating all the cervical vertebrae is expected.

In small animals, MRI is the first diagnostic tool of choice for detecting spinal disorders [14]. However, while one advantage of MRI is that it does not require a contrast agent, the limitation of MRI is that the size of the foal does not permit evaluation of the entire cervical vertebral column, even in an open type permanent magnet [7]. Furthermore, the field of view is also limited. Therefore, it is difficult to observe C1–7 in one sagittal image. Furthermore, the scan time for MRI is much longer compared with that of a CT scan. In summary, use of MRI for evaluation of the cervical spine in living horses is impractical. Indeed, previous studies on the equine cervical vertebra have reported performing a postmortem MRI [7, 12].

In conclusion, the stenosis ratios determined using CT myelography could be applicable for detecting primary lesion sites of the spinal cord.

Acknowledgments

This study was supported by a grant from the Equine Research Institute of the Japan Racing Association.

References

1. Aleman, M., Dimock, A.N., Wisner, E.R., Prutton, J.W., and Madigan, J.E. 2014. Atlanto-axial approach for cervical myelography in a Thoroughbred horse with complete fusion of the atlanto-occipital bones. *Can. Vet. J.* **55**: 1069–1073. [Medline]
2. Audigié, F., Tapprest, J., Didierlaurent, D., and Denoix, J.M. 2004. Ultrasound-guided atlanto-occipital puncture for myelography in the horse. *Vet. Radiol. Ultrasound* **45**: 340–344. [Medline] [CrossRef]
3. Barbee, D.D., Allen, J.R., and Gavin, P.R. 1987. Computed tomography in horses. *Vet. Radiol. Ultrasound* **28**: 144–151. [CrossRef]
4. DeLahunta, A., and Glass, E. 2009. Large animal spinal cord diseases. pp. 285–318. *In*: Veterinary Neuroanatomy and Clinical Neurology, 3rd ed., Saunders Elsevier, Philadelphia.
5. Hoffman, C.J., and Clark, C.K. 2013. Prognosis for racing with conservative management of cervical vertebral malformation in thoroughbreds: 103 cases (2002–2010). *J. Vet. Intern. Med.* **27**: 317–323. [Medline] [CrossRef]
6. Hughes, K.J., Laidlaw, E.H., Reed, S.M., Keen, J., Abbott, J.B., Trevail, T., Hammond, G., Parkin, T.D.H., and Love, S. 2014. Repeatability and intra- and inter-observer agreement of cervical vertebral sagittal diameter ratios in horses with neurological disease. *J. Vet. Intern. Med.* **28**: 1860–1870. [Medline] [CrossRef]
7. Janes, J.G., Garrett, K.S., McQuerry, K.J., Pease, A.P., Williams, N.M., Reed, S.M., and MacLeod, J.N. 2014. Comparison of magnetic resonance imaging with standing cervical radiographs for evaluation of vertebral canal stenosis in equine cervical stenotic myelopathy. *Equine Vet. J.* **46**: 681–686. [Medline] [CrossRef]
8. Levine, J.M., Adam, E., MacKay, R.J., Walker, M.A., Frederick, J.D., and Cohen, N.D. 2007. Confirmed and presumptive cervical vertebral compressive myelopathy in older horses: a retrospective study (1992–2004). *J. Vet. Intern. Med.* **21**: 812–819. [Medline]
9. Nout, Y.S., and Reed, S.M. 2003. Cervical vertebral stenotic myelopathy. *Equine Vet. Educ.* **15**: 212–223. [CrossRef]
10. Rose, P.L., Abutarbush, S.M., and Duckett, W. 2007. Standing myelography in the horse using a nonionic contrast agent. *Vet. Radiol. Ultrasound* **48**: 535–538. [Medline] [CrossRef]
11. Scrivani, P.V., Barthez, P.Y., Léveillé, R., Schrader, S.C., and Reed, S.M. 1997. Subdural injection of contrast medium during cervical myelography. *Vet. Radiol. Ultrasound* **38**: 267–271. [Medline] [CrossRef]
12. Sleutjens, J., Cooley, A.J., Sampson, S.N., Wijnberg, I.D., Back, W., van der Kolk, J.H., and Swiderski, C.E. 2014. The equine cervical spine: comparing MRI and contrast-enhanced CT images with anatomic slices in the sagittal, dorsal, and transverse plane. *Vet. Q.* **34**: 74–84. [Medline] [CrossRef]
13. Van Biervliet, J., Mayhew, J., and de Lahunta, A. 2006. Cervical vertebral compressive myelopathy: diagnosis. *Clin. Tech. Equine Pract.* **5**: 54–59. [CrossRef]
14. Wisner, E., and Zwingenberger, A. 2015. Intervertebral disk disease and other degenerative disorders. pp. 355–375. *In*: Atlas of Small Animal CT and MRI. 2015. Wiley-Blackwell, Oxford.